A. GÓRAL*,#, K. BERENT**, M. NOWAK***, B. KANIA*

MICROSTRUCTURE AND PROPERTIES OF Ni AND Ni/Al₂O₃ COATINGS ELECTRODEPOSITED AT VARIOUS CURRENT DENSITIES

The study presents investigations of an influence of various direct current densities on microstructure, residual stresses, texture, microhardness and corrosion resistance of the nickel coatings electrodeposited from modified Watt's baths. The properties of obtained coatings were compared to the nano-crystalline composite Ni/Al_2O_3 coatings prepared under the same plating conditions. The similarities and differences of the obtained coatings microstructures visible on both their surfaces and cross sections and determined properties were presented. The differences in the growth character of the Ni matrix and in the microstructural properties were observed. All electrodeposited Ni and Ni/Al_2O_3 coatings were compact and well adhering to the steel substrates. The thickness and the microhardness of the Ni and Ni/Al_2O_3 deposits increased significantly with the current density in the range 2 - 6 A/dm². Residual stresses are tensile and they reduced as the current density increased. The composite coatings revealed better protection from the corrosion of steel substrate than pure nickel in solution 1 M NaCl.

Keywords: Ni coating, Ni/Al_2O_3 composite coating, microstructure, corrosion resistance

1. Introduction

Nanocomposite coatings based on a metallic matrix with dispersed ultrafine/nano-particles of pure metals, ceramics or organic particles, have attracted much attention in recent years due to their unique physical, chemical and mechanical properties. Electrolytic nickel coatings exhibit favourable properties such as hardness, durability, good corrosion resistance and catalytic activity in many electrochemical processes [1]. Moreover, some properties could be improved by using nano-crystalline nickel substrate instead of a micro-crystalline one. Nickel, as a durable and tough metal, was widely used as a matrix in composites because it is resistant to corrosion and abrasion. The addition of hard ceramic particles into Ni matrix can improve its hardness and wear resistance. The most sought after method of producing pure Ni and Ni-based as well as Ni matrix composite coatings is electrodeposition, owing to its advantages like low cost and low process temperature [2]. Nickel electroplating is a commercially important and versatile surface finishing process. Some of the nickel-base alternatives (Ni-W, Ni-Mo, Ni-B, Ni-Co, etc.) [3-6] and nickel matrix composites reinforced with ceramic nano-particles (Al_2O_3, TiO_2, ZrO_2, SiC, etc.) [7-17] may be considered as candidates for replacement hard and decorative thin dense electrodeposited chromium coatings, which production has harmful impact on workers' health and the natural environment. Ni/Al_2O_3 coatings are interest of scientific researches to improve the nickel hardness and wear properties. However, the most important field of improvements is a choice of suitable electrodeposition parameters assuring obtaining coatings with good quality and nano-crystalline structure. Many interrelated experimental parameters influence the deposition process. A clear picture of the exact effect of each factor is difficult to obtain, because often different, or even contradicting results are reported by different authors. In general, electrodeposition parameters can be gathered into two groups: one is connected with a type of used solution (electrolyte concentration, additives, surfactant type), second one is related to plating process conditions (current density, temperature, pH value, bath agitation etc). In this paper the microstructure and chosen properties, such as microhardness, texture, residual stresses and corrosion resistance of Ni coatings obtained at different current densities were investigated and compared with nickel matrix coatings with the co-deposited α-Al_2O_3 nano-particles presented by Góral et al. [14]. The presented results enabled to compare some properties of pure Ni and Ni/Al_2O_3 (produced from Watt's bath into which 20 g/l of α-Al_2O_3 nano-particles were added) coatings obtained under the same electrodeposition parameters. In the literature we can find numerous papers characterising different electrodeposition products [7-13,18-19], but detailed statement of mentioned above properties for these coatings is still lacking.

2. Experimental details

The Ni coatings were electrodeposited from the modified Watt's bath containing: 120 g/l $NiSO_4 \cdot 6H_2O$, 70 g/l $NiCl_2 \cdot 6H_2O$, 50 g/l H_3BO_3 under the same conditions as Ni/Al_2O_3 coatings presented in reference [14] on steel substrates.

* INSTITUTE OF METALLURGY AND MATERIALS SCIENCE, POLISH ACADEMY OF SCIENCES, 25 REYMONTA STR., 30-059 KRAKOW, POLAND

** AGH UNIVERSITY OF SCIENCE AND TECHNOLOGY, ACADEMIC CENTRE FOR MATERIALS AND NANOTECHNOLOGY, AL. MICKIEWICZA 30., 30-059 KRAKOW, POLAND

*** INSTITUTE OF NON-FERROUS METALS GLIWICE, LIGHT METALS DIVISION SKAWINA, 19 PILSUDSKIEGO STR., 32-050 SKAWINA, POLAND

The examinations were taken for the coatings produced at direct current densities ranging from 2 A/dm^2 to 6 A/dm^2. Time of electrodeposition of all coatings was the same and amounted to 600 s. The microstructures and morphology of the Ni deposits were characterised by scanning electron microscope (FEI QUANTA 3D FEG). The phase composition, residual stresses and preferred grain orientation of the coatings were determined using X-ray diffraction techniques (Bruker D8 diffractometer with CoKα filtered radiation). Residual stresses of obtained coatings were measured based on Ni phase - {311} Ni reflection using sin^{2}ψ method in ψ - geometry [20]. Corrosion tests were carried out using potentiodynamic methods using an AUTOLAB PGSTAT model 302 device after 24 hours of immersion in corrosive solution (1 M NaCl) at the temperature of 25°C. The Ni specimen's working surface amounted to 2.8 cm^2. A saturated Ag/AgCl 3M KCl electrode was the reference electrode and a platinum electrode was the auxiliary electrode. The microhardness of the coatings was measured by Vicker's microhardness tester (Buehler Micromet 5103) with a load of 500 mN. At least eight indentations were made on the surface of each coating, and the values were then averaged.

3. Results and discussion

The nickel coatings electrodeposited at various current densities ranging from 2 A/dm^2 to 6 A/dm^2 had a rather similar geometry of surfaces. The surface morphology was characterized by trigonal pyramids, in contrast to the composite Ni/Al$_2$O$_3$ coatings, which rather developed a nodular surface structure [14]. Figure 1 presents the microstructure of surfaces and cross sections of coatings obtained at 2 A/dm^2 and 6 A/dm^2. The Ni pyramids visible on the surfaces of coatings became coarser when the current density was higher. The SEM images revealed all coatings were compact, smooth and well adhered to steel substrates without any pores and cracks on the surfaces. The effect of the current density on the coating thickness is illustrated in Fig 1.b,d. Electrodeposition time of all coatings was the same. It is clear from cross section observations that the actual thickness of the coatings depended on the applied current density and increased with its value. The thicknesses of coatings produced at 2 A/dm^2, 3 A/dm^2, 4 A/dm^2, 5 A/dm^2 and 6 A/dm^2 measured in SEM on their cross sections were about 3.7 μm, 3.9 μm, 4.3 μm, 7.0 μm and 7.8 μm, respectively. The similar effect was also observed for Ni/Al$_2$O$_3$ coatings, but they were thinner (2.5 - 6.6 μm) [14] compared to the pure Ni coatings obtained at the same current density. It is seen that the coating thickness increases with the increasing current density. However, obtained results suggest that incorporated particles restrain nickel growth and the Ni grains stop growing when they come across the ceramic nano-particles.

In order to better understand an influence of the direct current density on properties obtained coatings, a changes of crystallographic texture of Ni was also examined.

The texture of Ni coatings was determined based on the experimental pole figures {200}, {220} and {311} measured by XRD technique, as well as additional (APF) pole figures calculated from orientation distribution functions, similar as in the case of the Ni/Al$_2$O$_3$ coatings [14]. The pure Ni coatings obtained at the lower current densities revealed the strong {112}<uvw> and soft {001}<uvw> axial texture components. However, the intensity of {001}<uvw> increased with the increasing current density. In the coatings deposited at the biggest current density most Ni grains showed strong {001}<uvw> and little of them - soft {112}<uvw> preferred crystallographic orientation. The same relationships between current density and observed texture were also determined in the Ni/Al$_2$O$_3$ coatings [14]. These results indicated the change of the current density influenced the preferred crystallographic orientations both in the pure Ni and composite Ni/Al$_2$O$_3$ coatings.
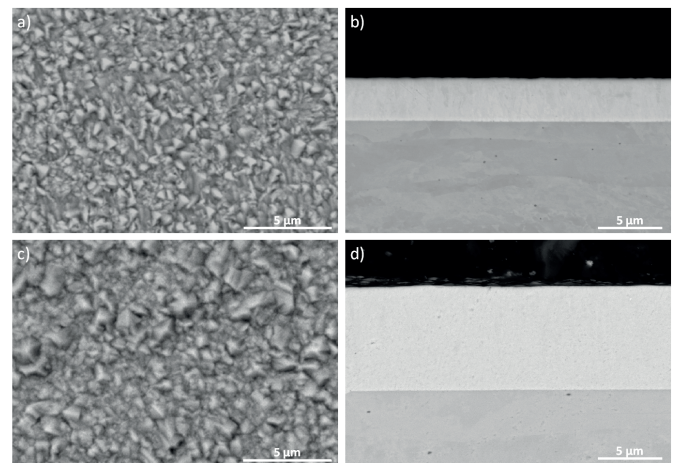

Fig.1. SEM images of surfaces and cross sections of Ni electrodeposits obtained at various current density: 2 A/dm^2 (a, b) and 6 A/dm^2 (c, d)

In turn, to test the current density dependence on mechanical properties the microhardness was measured in eight places on the surface of each samples. The microhardness values of the deposited Ni coatings at different current densities are presented in Tab. 1. It can be found that microhardness of coatings increased (from 207 to 267 HV0.05) with increasing thickness (from 3.7 to 7.8 μm) and current density. Although the size of surface roughness in terms of "trigonal pyramids" increases versus current density, microhardness confirms inverse relation i.e. decrease of grain/subgrain microstructure when current density increases. The microhardness value of Ni/Al$_2$O$_3$ composite was higher compared to pure Ni coating at entire current densities. Additionally, it can be seen that microhardness values of Ni/Al$_2$O$_3$ coatings were approximately 10-15% higher than coatings without ceramic phase (Tab. 1).

As can be seen in Tab. 1 determined residual stresses of Ni coatings are tensile and their values reduced as the current density increased. The estimated values were approximately the same (in the range of estimated uncertainty) as that of composite coatings.
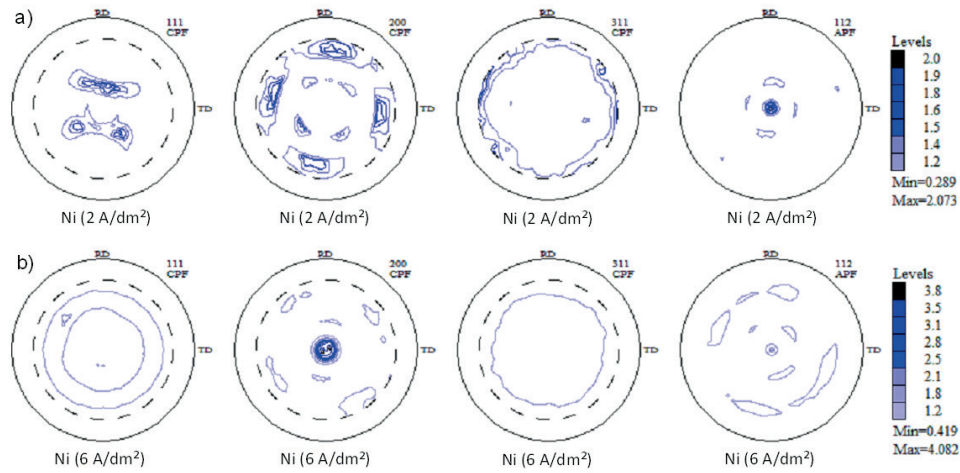
Fig. 2. Experimental (CPF) {200}, {220}, {311} and additional (APF) {112} pole figures of the Ni coatings obtained at the current density: 2 A/dm² (a) and 6 A/dm² (b). APF {112} pole figure was calculated from orientation distribution function created on the basis of CPF.

TABLE 1

Residual stresses and microhardness determined in Ni and Ni/Al$_2$O$_3$ [14] coatings

Current density [A/dm²]	Ni coatings		Ni/Al$_2$O$_3$ coatings	
	Residual stresses [MPa]	Microhardness HV0.05	Residual stresses [MPa]	Microhardness HV0.05
2	345 ± 30	207 ± 3	342 ± 18	233 ± 8
3	325 ± 30	223 ± 5	313 ± 16	246 ± 11
4	290 ± 30	239 ± 2	261 ± 12	260 ± 8
5	280 ± 25	244 ± 2	286 ± 8	265 ± 6
6	225 ± 25	267 ± 3	258 ± 8	300 ± 4

The structural differentiation of pure Ni and Ni/Al$_2$O$_3$ coatings induced also the changes in their protective properties and the mechanism of the corrosion destruction. The potentiodynamic polarization curves of examined Ni coatings were recorded after 24 h of exposure of the specimens in the 1 M NaCl solution. The E$_{corr}$ and I$_{corr}$ values were calculated using the Tafel extrapolation method [21] and values are given in Tab. 2. There is an appreciable increase in corrosion resistance for both Ni and Ni/Al$_2$O$_3$ coatings with increasing current density. However, the E$_{corr}$ values measured under the same conditions showed some differences between the two types of coatings. As can be seen from Tab. 2. the starting value of corrosion potential is more negative for pure nickel coating; E$_{corr}$ = −851 mV, than that for composite Ni/Al$_2$O$_3$; E$_{corr}$ = −823 mV. With an increase in the current densities the value of corrosion potential became more positive for Ni coatings which is accompanied by the increase in polarization resistance.

The corrosion resistance of the standard nickel coating increased with the increasing current density. However, it is significantly lower than that of the Ni/Al$_2$O$_3$ coatings, especially in the case of the sample obtained at 5 A/dm², which has corrosion resistance almost 5 times higher than that of composite coating. Among the pure Ni coatings the highest anticorrosion performance was exhibited by the coatings obtained at 6 A/dm², whereas for composites - coatings obtained at 5 A/dm². The increasing current density causes further decrease in corrosion current density in Ni coating indicating better corrosion resistance in 1 M NaCl environment (Tab. 2).

SEM observations showed several localized corrosion pits on each coating surface after polarization measurements. An exemplary microstructure of the surface and the cross section of the deposits with visible corroded area is presented in Fig. 3. An interesting morphological feature of these pits is their almost circular shape, a fact often reported when pitting corrosion occurs on different metal surfaces. An area presented in Fig. 3c shows a corrosion way of the coating - substrate system visible on the cross section. Examinations on the Ni coating cross section revealed the corrosion pit in the coating, which penetrated to the substrate surface. It can be seen a region where the pitting corrosion was initiated presenting continuous length of the coating under which the corroded area of steel substrate is shown. However, a comparison of those areas enables to state that destructed substrate area adjacent directly to the coating was significantly larger than that occurring in the coating.

TABLE 2

The results of potentiodynamic measurements for Ni coatings in 1 M NaCl solution set with the results obtained for Ni/Al$_2$O$_3$ coatings [14]

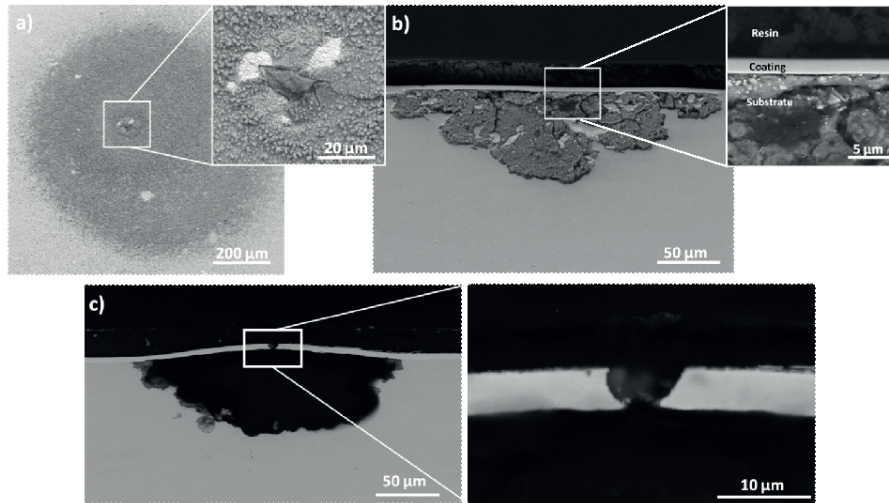| Current density [A/dm²]	Ni coatings			Ni/Al$_2$O$_3$ coatings		
	icorr [A/cm²]	Rp [Ω]	Ecorr [mV]	icorr [A/cm²]	Rp [Ω]	Ecorr [mV]
2	3,81·10-5	610	-851	1.14·10-5	722	-823
3	3,64·10-5	665	-808	2.04·10-5	1132	-852
4	2,40·10-5	686	-797	1.17·10-5	2939	-768
5	2,23·10-5	681	-795	4.37·10-6	3202	-622
6	2,17·10-5	706	-797	1.05·10-5	1821	-827

Fig. 3. An example of the corroded surface and the cross section of the Ni deposits

In the case of nanocomposite coatings the effective metallic area prone to corrosion is decreased and the corrosion process proceeds in the different way than in pure Ni, it has not been observed the drastic substrate destruction. The examinations revealed that the corrosion went from the coating surface far into it (Fig. 4). Incorporating more oxide particles in the deposits induces a higher resistance against the corrosion of these layers. The α-Al_2O_3 particles co-deposited with the nickel are new nucleation sites for Ni grains and they change the microstructure of nickel from coarse-grained columnar to fine-grained granular structure, so that corrosion can only proceed along less straight paths due to changing of grain boundaries [16]. Also, α-Al_2O_3 particles act as inert physical barriers to the initiation and development of corrosion which contributes to isolating corrosive medium, decreasing corrosive area and increasing corrosion resistance.
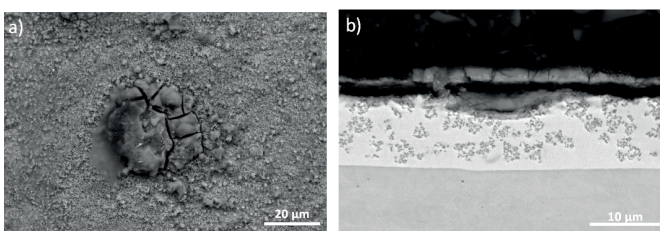

Fig. 4. The exemplary microstructure of the Ni/Al_2O_3 composite coating obtained at 6 A/dm^2 after corrosion tests: surface (a), cross section (b)

4. Conclusions

The paper presents how the changes of current density influence the microstructure, residual stresses, texture, microhardness and corrosion properties of pure Ni coatings. The results were compared to the composite Ni/Al_2O_3 coatings obtained from the Watt's bath containing 20 g/l α-Al_2O_3 nano-powder. It was shown that this parameter affects all mention above characteristics to a greater or lesser degree:

1. The thickness of the Ni and Ni/Al_2O_3 deposits increased significantly with applied current density, the microhardness showed the similar tendency. However, it was observed the thickness of Ni/Al_2O_3 deposits was lower than that of pure Ni obtained under the same conditions.
2. The texture of Ni grains of all coatings without and with addition of α-Al_2O_3 nano-particles was changed from {112}<uvw> to {100}<uvw>.
3. The residual stresses of coatings stayed at the same level (in the uncertainty range) and they were reduced as the current density increased.
4. The corrosion resistance of the standard nickel coating increased with the increasing current density. The finer grain structure of composite coatings with nano-Al_2O_3 particles embedded in Ni matrix decreases speed of the corrosion process and improves the corrosion resistance. Additionally, the microstructures of cross sections of coatings after 24 h exposure in corrosive solution showed that the composite coatings give better protection from the corrosion of steel substrate than pure nickel.

REFERENCES

[1] Technical Tidbits a publication by BRUSH WELLMAN ENGINEERED MATERIALS vol. **4**, 4 (2002).

[2] A. Góral, J.Deda E. Bełtowska-Lehman, B. Major, Analysis of Strengths, Weaknesses, Opportunities and Threats (SWOT) and Prerequisite Tree (PT) of Selected Technologies for Coating and Layer Production. Arch Metall Mater **53**, 979-984 (2008).

[3] J. Du, L. Xu, B. Chen, L. De, Electrodeposition of nanocrystalline Ni-W coatings with citric acid system, J Nanosci Nanotechnol **13**, 690-693 (2013).

[4] P. Prioteasa, L. Anicai, T. Visan, Synthesis and corrosion characterization of electrodeposited Ni-Mo alloys obtained

from aqueous solutions, U.P.B. Sci Bull B **72**, 11-24 (2010).

[5] H. Zhang, X. J. Zhang, Y. K. Zhang, Structure and Properties of electroless Nickel-Boron alloys, Plat Surf Finish **80**, 80-84 (1993).

[6] M. Srivastava, V.K. William Grips, K.S. Rajam, Electrochemical deposition and tribological behaviour of Ni and Ni-Co metal matrix composites with SiC nano-particles, Appl Surf Sci **253**, 3814-3824 (2007).

[7] M. Verest, J.P. Bonino, M. Brieu, A. Rouset, Thermomechanical properties of Ni-Al2O3 metal matrix composites produced by electroforming, Mat Sci Eng A **191**, 165-169 (1995).

[8] S.T. Aruna, V. Ezhil Selvi, V.K. William Grips, K.S. Rajam, Corrosion- and wear-resistant properties of Ni-Al2O3 composite coatings containing various forms of alumina, J. Appl Electrochem **41**, 461-468 (2011).

[9] H. Gul, F. Kilic, S. Aslan, A. Alp, H. Akbulut, Characteristics of electro-co-deposited Ni-Al$_2$O$_3$ nano-particle reinforced metal matrix composite (MMC) coatings, Wear **267**, 976-990 (2009).

[10] A.B. Vidrine, E.J. Podlaha, Composite electrodeposition of ultrafine γ-alumina particles in nickel matrices. Part I: Citrate and chloride electrolytes, J. Appl Electrochem **31**, 461-468 (2001).

[11] X.Y. Wei, Z.G. Zhu, P.D. Prewett, K. Jiang, Fabrication of Ni-Al2O3 composite microcomponent by electroforming, Microelectron Eng **84**, 1256-1259 (2007).

[12] S-L.Kuo, Y-C. Chen, M-D. Ger, W-H. Hwu, Nano-particles dispersion effect on Ni/Al$_2$O$_3$ composite coatings, Mater

[13] I. Corni, R.J. Chater, A.R. Boccaccini, Electro co-deposition of Ni-Al$_2$O$_3$ composite coatings, J. Mater Sci **47**, 5361-5373 (2012).

[14] A. Góral, M. Nowak, K. Berent, B. Kania, Influence of current density on microstructure and properties of electrodeposited nickel-alumina composite coatings. J Alloy Compd **615**, S406-S410 (2014).

[15] G. Parida, D. Chaira, M. Chopkar, A. Basu, Syntesis and characterization of Ni-TiO$_2$ composite coatings by electro-co-deposition, Surf Coat Tech **205**, 4871-4879 (2011).

[16] R. Arghavanian, N. Parvini-Ahmadi, The effect of co-electrodeposited ZrO$_2$ particles on the microstructure and corrosion resistance of Ni coatings, J Solid State Electrochem **15**, 2199-2204 (2011).

[17] I. Garcia, A. Conde, G. Langelaan, J. Fransaer, J.P. Celis, Improved corrosion resistance through microstructural modifications induced by codepositing SiC-particles with electrolytic nickel, Corros Sci **45**, 1173-1189 (2003).

[18] R.K. Saha, T.I. Khan, Effect of applied current on the electrodeposited Ni-Al$_2$O$_3$ composite coating, Surf Coat Tech **205**, 890-895 (2010).

[19] B. Szczygiel, M. Kolodziej, Corrosion resistance of Ni/Al$_2$O$_3$ coatings in NaCl solution, T I Met Finish **83**, 181-187 (2005).

[20] S. Skrzypek, A. Baczmański, W. Ratuszek, E. Kusior, New approach to stress analysis based on grazing incidence X-ray diffraction, J Appl Crystallogr **34** 427-435 (2001).

[21] Autolab-Application Note no 016

Chem Phys **86**, 5-10 (2004).